ISBN: 978-3-95450-234-9 ISSN: 2673-5504 doi:10.18429/JACoW-SRF2023-TUPTB069

DESIGN AND TESTS OF A CATHODE STALK FOR THE LCLS-II-HE LOW EMITTANCE INJECTOR SRF GUN*

T. Konomi†, W. Hartung, S. Kim, S. Miller, D. Morris, K. Saito, A. Taylor, Z. Yin, T. Xu
Facility for Rare Isotope Beams, Michigan State University, East Lansing, MI, USA
M. Kelly, T. Petersen, Argonne National Laboratory, Argonne, IL, USA
C. Adolphsen, J. Lewellen, J. Smedley, SLAC National Accelerator Laboratory, CA, USA
S. Gatzmanga, P. Murcek, R. Xiang, Helmholtz Zentrum Dresden Rossendorf, Dresden, Germany

Abstract

A superconducting radio-frequency photo-injector can in principle operate CW with a high cathode gradient and ultra-low vacuum for high-quantum efficiency, low MTE photocathodes, useful features for delivery of high-brightness, high-repetition-rate beams. For these reasons, an SRF based photoinjector was chosen for the proposed Low Emittance Injector (LEI) addition to the Linac Coherent Light Source II High-Energy Upgrade (LCLS-II-HE) facility, which will operate CW with bunch rates up to 1 MHz. For this injector, a prototype 185.7 MHz quarter-wave resonator gun is being developed in a collaborative effort among FRIB, HZDR, ANL and SLAC with the goal of achieving a photocathode gradient of at least 30 MV/m. The photocathode will be held by a coaxial fixture ("cathode stalk") for thermal isolation from the cavity body. The system must allow for precise alignment of the photocathode, particle-free photocathode exchange, cryogenic (55-70 K) or warm (273-300 K) photocathode operating temperatures, and DC biasing to inhibit multipacting. A prototype cathode stalk has been built and bench tests are underway to validate the design. Measurements include RF power dissipation, DC bias hold-off, multipacting suppression and heat transfer effectiveness. This paper describes the cathode stalk design and the test results.

INTRODUCTION

The Linac Coherent Light Source II High Energy (LCLS-II-HE) Project at SLAC has designed a Low-Emittance Injector (LEI) that employs a quarter-wave resonator (QWR) type superconducting radio-frequency (SRF) cavity as the electron source [1, 2]. The cavity frequency is 185.7 MHz, one-seventh of the 1.3 GHz LCLS-II-HE linac frequency. The advantage of using a low frequency SRF cavity is that it can provide a quasi-DC field in the accelerator gap and operate efficiently at 4 K. A prototype gun cryomodule is being developed in a collaboration among FRIB, ANL, HZDR and SLAC [3-5]. One of the critical parameters to achieve high-brightness bunches is the cathode gradient. The goal of the gun R&D program is to demonstrate stable CW operation with a cathode gradient of at least 30 MV/m.

The cathode stalk that holds the cathode plug is shown in Fig. 1. The plug and its insertion mechanism, and the stalk positioning mechanism, are based on those used in HZDR's 1.3 GHz SRF gun [6]. The coaxial section between the outer stalk and the cavity cathode tube can be DC biased up to 5 kV for multipacting (MP) suppression. Cooling tubes that connect to the plug holder will allow the plug to be maintained at 300 K or 55 K [7, 8] during gun operation: helium gas will be used as the coolant.

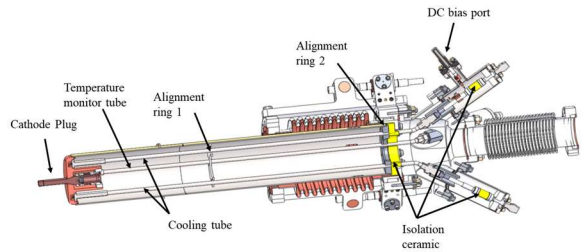

Figure 1: Cathode Stalk assembly [7].

RF/DC TEST SETUP

To demonstrate the cathode stalk temperature control and MP suppression, the RF/DC test setup shown in Fig. 2 was built [7]. The setup includes an RF-driven coaxial resonator that generates fields in the stalk coaxial region similar to those during gun operation. The resonator and stalk are installed into a vacuum chamber and pumped through slits on outer conductor and cathode stalk. The vacuum chamber has a monitor port to inset optical temperature sensors and a plug tip heater.

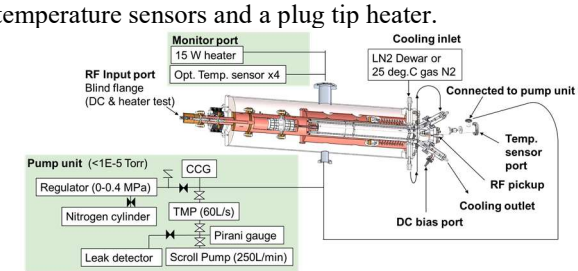

Figure 2: RF/DC test setup [7].

HEATER TEST

The thermal contact resistance between the plug and holder needs to be low to prevent the plug from over-heating. A heater test was done to verify this. The resonator and RF input coupler were removed for this test and the input port was closed with a blank flange. The holder and upstream stalk flange were cooled with dry nitrogen gas or liquid nitrogen. The cathode plug was inserted into the cone-shaped socket in the plug holder and held in place by an Inconel spring mechanism, the same as in the HZDR

* Work supported by the Department of Energy under Contract DE-AC02-76SF00515
† konomi@frib.msu.edu

ISBN: 978-3-95450-234-9 ISSN: 2673-5504 doi:10.18429/JACoW-SRF2023-TUPTB069

gun. The heater and optical temperature sensors were configured as shown in Fig. 3. Apiezon N cryogenic high vacuum grease was used to achieve good thermal contact. Data were acquired for different heater power levels after allowing sufficient time (~ 1 hour) for the temperature to stabilize. Figure 4 shows the temperature difference between the plug and holder versus heater power; the slope is essentially independent of the operation temperature. Fitting a line through zero point yields a thermal conductivity is 0.9 K/W, which is similar to the HZDR result from a test they did for their gun [9]. This value is 20% less than the design target in the gun cryomodule test plan.

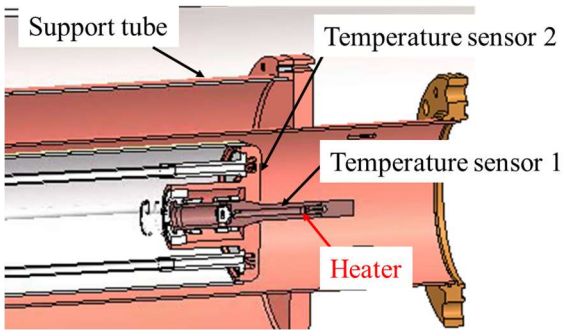

Figure 3: Heater test setup: layout of the heater and temperature sensors.

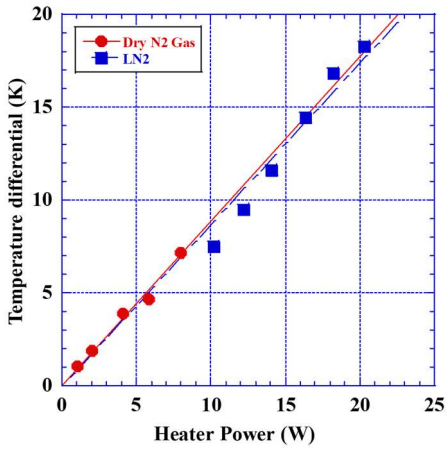

Figure 4: Temperature difference between the cathode plug and holder with dry nitrogen gas and liquid nitrogen cooling.

OPTIMIZING CABLE LENGTH OF CHOKE FILTER

A choke filter will be located inside the gun cryomodule to prevent RF power from reaching the DC bias voltage supply. The choke filter consists of a fixed inductor (Bourns Inc., 5230-RC) and a shielded box (Pomona Electronics Inc., model: 2902 with SHV connector). Figure 5 shows the S-parameter measurements of the choke filter at room and liquid nitrogen temperature, and the simulated room temperature response of the ferrite core. The isolation (S21) at 185.7 MHz is about -30 dB at both room and liquid nitrogen temperatures.

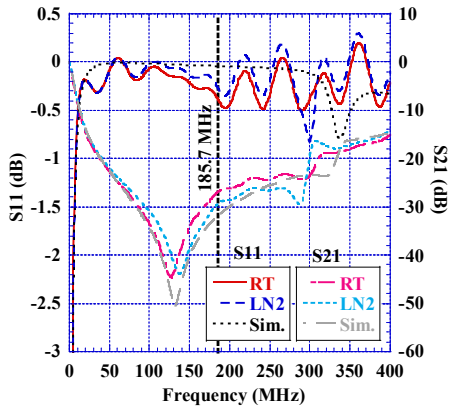

Figure 5: S-parameters of the choke filter at room temperature and liquid nitrogen temperature.

It is also necessary to optimize the cable length from the DC port on the stalk to the choke filter to minimize RF losses in the cable. As a test, the filter was connected to the stalk port via a series of coaxial trombone phase shifters and a long cable, and the filter was terminated in a 50-Ohm load. Figure 6 shows the measured test setup Qo values and frequencies versus the total coaxial length. The resonator had not yet been tuned at this time, and the frequency and Qo were 190.5 MHz and 450, respectively, with an open condition at the stalk DC port. As expected, the maximum Qo values occurred every half wavelength where the frequency equals that with the open port. The Qo loss from the cable was less than 10%. As a result, we decided to use a 3/4 wavelength cable for the test setup and gun cryomodule.

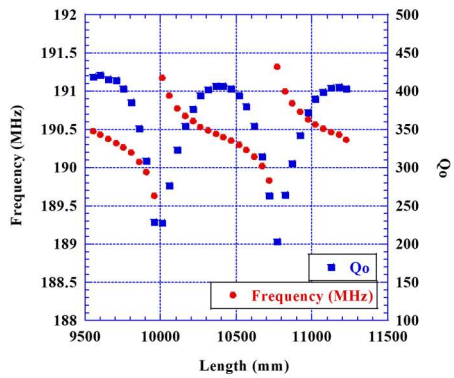

Figure 6: Qo values and frequencies versus total coaxial length (RF half-wavelength ~ 800 mm).

HIGH POWER TEST

During high power operation, an equivalent cathode field strength was computed based on the energy stored in RF/DC test setup, which was inferred from the power balance as measured with the power meters shown in Fig. 7. The loaded Q was derived from the bandwidth measured by sweeping the frequency at low power, and the resulting Qt was used to compute Qo at high power. The current through DC bias port was monitored using a 1 MΩ resister in series with the HV cable. This current monitor served as a MP indicator as did the cold cathode gauge (CCG) pressure monitor.

ISBN: 978-3-95450-234-9 ISSN: 2673-5504 doi:10.18429/JACoW-SRF2023-TUPTB069

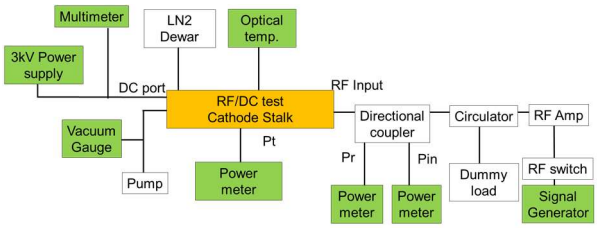

Figure 7: Layout for the RF/DC test at high power.

The RF parts of RF/DC test setup were assembled after ultrasonic rinsing of each component in a clean bath. No baking was performed after assembly. Figure 8 shows high power test results with a DC bias voltage of -1 kV. The plug holder and upstream flange were cooled with dry nitrogen gas at room temperature or liquid nitrogen. Qo increased from 450 to 1000 at the lower temperature and the resonant frequency increased from 188.5 to 189.5 MHz.

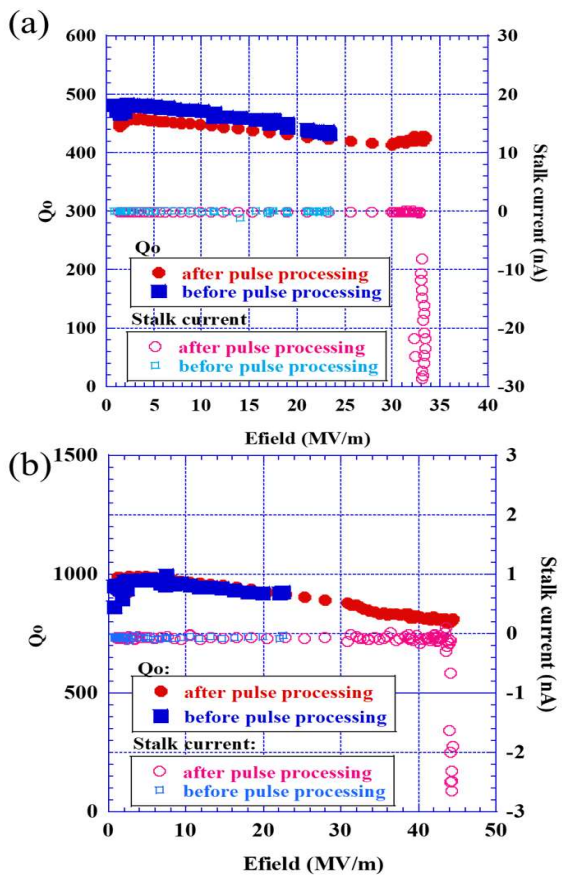

Figure 8: High power test results. The cathode stalk and flange were cooled with (a) dry nitrogen gas or (b) liquid nitrogen.

Before the 'after processing' data shown in Fig. 8 was taken, 1 Hz pulsed processing had been performed for approximately 1 hour during which the pulse width was increased from 50 ms to 600 ms. This improved the gradient reach: 33 MV/m at room temperature and 44 MV/m at liquid nitrogen temperature, each limited by the available power (100 W) from the RF amplifier.

DC BIAS VOLTAGE

Figure 9 shows the maximum gradient versus DC bias voltage at room temperature after pulse processing. A maximum gradient of 30 MV/m was achievable at bias voltages below –250 V and above +400 V. In Ref. [10], these data are compared to simulation results.

A bias voltage of 5 kV was applied with the RF off using a high potential tester (Hipot). No dark current was observed above the 100 nA lower limit of the tester.

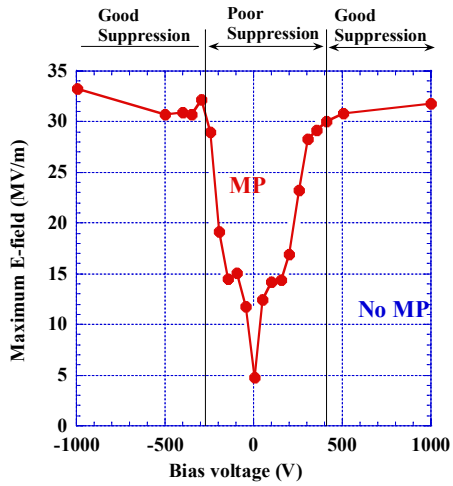

Figure 9: Maximum gradient versus bias voltage at room temperature after pulse processing.

SUMMARY

An RF/DC test setup was built to evaluate the SRF gun cathode stalk performance. The first round of tests showed that the cathode stalk design meets the functional requirements. In particular, the cooling scheme functioned as designed and the cathode plug thermal contact conductivity was as expected. The DC bias RF choke filter was effective and the length of its cable connection was optimized. No MP was observed up to an effective cathode gradient of 44 MV/m after pulse processing. No significant dark current was observed up to DC bias voltage of 5 kV.

ACKNOWLEDGEMENTS

This work supported by the Department of Energy Contract DE-AC02-76SF00515.

REFERENCES

[1] "LCLS-II-HE Low Emittance Injector Conceptual Design Report", Tech. Rep. LCLS-II-HE-1.1-DR-0418-R0, Mar. 2022.

[2] J. W. Lewellen *et al.*, "Status of the SLAC/MSU SRF Gun Development Project", in *Proc. NAPAC'22*, Albuquerque, NM, USA, Aug. 2022, pp. 623-626. doi:10.18429/JACoW-NAPAC2022-WEPA03

[3] T. Xu *et al.*, "Low-emittance SRF photo-injector prototype cryomodule for the LCLS-II high-energy upgrade: design and fabrication", presented at the IPAC'23, Venice, Italy, May 2023, paper TUPA028.

[4] S. H. Kim *et al.*, "Design of a 185.7 MHz Supercon-ducting RF Photoinjector Quarter-Wave Resonator for the LCLS-II-

ISBN: 978-3-95450-234-9 ISSN: 2673-5504 doi:10.18429/JACoW-SRF2023-TUPTB069

HE Low Emittance Injector", in *Proc. NAPAC'22*, Albuquerque, NM, USA, Aug. 2022, pp. 245-248. doi:10.18429/JACoW-NAPAC2022-MOPA85

[5] S. Miller *et al*., "Status of the SLAC/MSU SRF Gun Development Project", presented at SRF'23, Grand Rapids, MI, USA, Jun. 2023, paper FRIBA07, this conference.

[6] J. Teichert *et al*., "Successful user operation of a superconducting radio-frequency photoelectron gun with Mg cathodes", *Phys. Rev. Accel. Beams*, vol. 24, p. 033401, 2021.

[7] T. Konomi *et al*., "Design of the Cathode Stalk for the LCLS-II-HE Low Emittance Injector", in *Proc. NAPAC'22*, Albuquerque, NM, USA, Aug. 2022, pp. 253-255. doi:10.18429/JACoW-NAPAC2022-MOPA87

[8] R. Xiang *et al*., "Design of a Cathode Insertion and Transfer System for LCLS-II-HE SRF Gun", presented at SRF'23, Grand Rapids, MI, USA, Jun. 2023, paper MOPMB067, this conference.

[9] A. Arnold, "Solving overheating of Cs2Te cathodes in the ELBE SRF gun", presented at 7th annual meeting of the programme "Matter and Technologies" of Helmholtz Association, Deutschland (virtual), Feb.2021.

[10] Z. Yin *et al*., "Evaluation of Photo-cathode port Multipacting in the SRF photo-injector cryomodule for the LCLS-II High-Energy upgrade", presented at SRF'23, Grand Rapids, MI, USA, Jun. 2023, paper SUSPB032, this conference.